NUMERICAL INVESTIGATIONS IN THREE-DIMENSIONAL INTERNAL FLOWS

SEMI-ANNUAL STATUS REPORT

1 JANUARY THROUGH 30 JUNE 1991

Prepared for:

NASA-AMES RESEARCH CENTER

MOFFETT FIELD, CA 94035

UNDER NASA GRANT

NCC 2-507

By:

WILLIAM C. ROSE

ENGINEERING RESEARCH AND DEVELOPMENT CENTER

UNIVERSITY OF NEVADA, RENO

RENO, NV 89557

I. BACKGROUND

In 1990 NASA initiated its Generic Hypersonics Research Program (GHP). The general objectives of this research program are to develop technology background required for aeronautical research in the hypersonic Mach number flow range. These research efforts are to complement the National Aerospace Plane (NASP) program and are geared to the development of experimental and computational fluid dynamics techniques. Previous experience under the current research using the two-dimensional full Navier-Stokes code (SCRAM2D) has indicated the desirability of producing highly contoured internal portions of a hypothetical Mach 10 inlet. These results were presented in the previous progress report. The two-dimensional code was used in a parametric sense to design the contours for a specific Mach 10 hypersonic inlet. Flow conditions hypothesized to enter the inlet were taken from the experimental conditions available in the NASA-Ames 3.5 foot hypersonic wind tunnel. The 2D code has been used parametrically as a design tool because of its reasonable results, ease of use and relatively short computer turn around time.

The effects that potential three-dimensional effects might have on such an inlet designed with the two-dimensional code remain unknown. The purpose of the present report is to describe the application of the three-dimensional full Navier-Stokes code (SCRAM3D) to investigating the three dimensional flow fields that arise when swept sidewalls are added to the two-dimensional compression lines obtained in the previous portions of the present research effort.

II. INTRODUCTION

It is usually assumed for vehicles operating in the atmosphere above Mach numbers of about 5 that the propulsion system will be highly integrated with the overall vehicle. Because of the high temperature limitations of existing materials, control of the thick viscous boundary layer entering the propulsion path as a result of the highly integrated forebody is expected to have limited practical application at the high cruise Mach numbers. Thus it is desirable to develop an understanding of the flow fields expected to occur in such an integrated inlet system. At the high Mach numbers handling the thick boundary layers may be relatively easy due to their higher momentum content. However, as the Mach numbers decrease it is known that even the turbulent boundary layer will become more liable to separation and potential implications of inlet operability arise. For these cases, boundary layer bleed (below Mach numbers of about 5) may be required as part of the inlet operating procedure. However, for purposes of the present investigation, we concentrate on the cruise Mach number (assumed to be 10), and no boundary layer bleed is considered here.

In the previous progress report, various designs were arrived at using the SCRAM2D code. All of the designs have a geometry that is similar to the one shown in Figure 1 which is repeated from the previous report. The specific geometry shown in Figure 1 is noted as Mod. 23 and has a 10 degree compression forebody simulation section followed by two 4 degree ramps that nominally produce a coalescent shock wave system just ahead of the cowl lip. The specific case shown in Figure 1 also has a straight cowl with a slightly rounded ramp shoulder and a straight, constant area throat. This geometry produces a 36 degree total geometric turning angle. Another version studied extensively was one having a 28

degree total geometric turning angle, which was produced by having only one 4 degree compression on the ramp surface. Flow fields calculated from the 2D code for the inlet shown in Figure 1 are shown in Figure 2, and indicate the difficulties that occur in obtaining a smooth pressure distribution in the throat without contouring of the internal flow surfaces. Figure 3 shows the flow field that results when both cowl contouring and ramp contouring are used. It was shown in the previous study that contours such as these tend to produce more uniform flow fields in shorter throat (isolator) regions than without contouring. These results are repeated from the previous progress report. New efforts are discussed below.

Similar improved flow field behavior was found to result with the contoured ramp and cowl surfaces for the 28 degree geometric turning angle (Mod. 26G) as shown in Figure 4. The two-dimensional contour used in Figure 4 is the one chosen for the three-dimensional study, since the pressure rises are lower than the 36 degree case shown in Figure 3 and are more representative of those required for a realistic flight environment. The design Mach number of 10 was used also in the 3D study.

The Mach 10 design value was chosen to be a leap in the required technology beyond that developed in the NASP "Mach 5" inlet study. The Mach number of 10, on the other hand, is still low enough so that real gas/air chemistry issues such as dissociation and ionization are not expected to be the dominant issue in establishing the performance of the inlet either in ground-based simulations or in flight along NASP-like trajectories (approximately 2,000 psf dynamic pressure). These facts allow us to continue using the full Navier-Stokes codes, both SCRAM2D and SCRAM3D without the additional complexity

of air chemistry and the associated increases in computational time required to achieve numerical simulations of these flow fields.

III. RESULTS AND DISCUSSION

The two-dimensional compression contours shown for the solution in Figure 4 were applied to a three-dimensional grid having 301 points in the streamwise direction by 61 points across the two-dimensional compression direction by 31 points in the spanwise direction. The inlet was assumed to be symmetrical and have a half-width of 0.20 meters. The sidewalls of the grid were assumed to originate at the leading edge of the 10 degree compression ramp and terminate at the lip of the cowl. Figure 5 shows the perspective view of the inlet geometry with the ramp at the top, the center plane of the inlet shown to the left side with the sidewall to the right and the cowl in the lower portion of the figure. Flow is assumed to be from right to left in this figure. The cross-flow planes shown contain the Mach number contours from the three-dimensional solution obtained in the present study. Figure 6 adds the Mach number contours on the center plane of the inlet.

For modular installations, adjacent inlets share sidewalls. On the other hand, for purposes of wind tunnel testing, usually an isolated inlet is considered. For purposes of computational consideration, these two situations distinguish themselves primarily by either having an outboard ramp, that is a ramp beyond the sidewall, or not having an outboard ramp. In the present study, these two cases were examined with the multi-block SCRAM3D code for treating both the flow outboard of the sidewall as well as below the edge of the sidewall. Figure 7 shows the Mach number contours in a cross flow plane just ahead of the

cowl lip for the case having an outboard ramp similar to the multi-module installation. Little flow migrates across the sidewall, since the sidewall plane acts like a plane of symmetry. A large sidewall vortical feature (characteristic of ramp compression inlets with sidewalls) is seen (2). There is less tendency of the flow to spill over the sidewall (1). Due to the large displacement effect of the vortical feature on the flow field, both the initial and second ramp shock waves are bowed in the region of the sidewall. The flow field behavior shown in this figure is in contrast to that shown in Figure 8.

In Figure 8, the solution is shown at the same streamwise station as in Figure 7, however, for this case the outboard ramp has been removed so that the three-dimensional simulation is similar to that expected for an isolated inlet model as tested in a wind tunnel. In this case, the lower pressure associated with the freestream of the wind tunnel is allowed to exist on the outer boundaries of the solution. With this lower pressure outboard of the sidewalls (1), large spillage occurs over the sidewalls ahead of the cowl lip (2). This spillage tends to reduce (but not eliminate) the size of the vortical feature that is ultimately ingested into the internal portion of the inlet. This also results in the ramp shock wave having a slightly shallower angle along the sidewall, as can be seen in Figure 8.

In previous 3D studies, the sidewall flow fields have been shown to cause large perturbations to the internal flow fields, while the center portions of such inlets remain nominally two-dimensional. The differences between the two-dimensional and three-dimensional surface pressure distributions (from the center plane of the inlet) are shown in Figure 9. Some minor differences occur; however, the overall compression achieved along

the center line of the 3D solution is quite similar to that obtained with the 2D solution. Figure 10 shows a cross flow plane mass flow profile obtained at the exit of the inlet (around 2.0 meters). Here, the nominally two-dimensional portion of the inlet flow is seen clearly, while the flow near the sidewall shows the remnants of the sidewall vortex as has been acted on by the cowl shock wave and subsequent internal compressions.

The effect of three-dimensional flow fields on inlet performance is of interest. For purposes of comparison, Table 1 shows the mass-averaged total pressure recovery for the 2D and 3D calculations at three streamwise positions: forward of the cowl shock, just aft of the cowl shock, and near the exit of the inlet (denoted by the term "throat"). The magnitudes of the total pressure recoveries are not as significant as the differences between the 2D and 3D calculations as one goes through the inlet. For the overall recovery at the exit of the inlet, the ratio of the two-dimensional to three-dimensional calculated values is 1.31. This says that by doing 2D calculations alone one is likely to overestimate the inlet's performance when compared with that calculated with the 3D code (having the losses associated with the sidewall vortical flow and its interaction throughout the internal flow portion of the inlet).

	FORWARD OF COWL SHOCK	AFT OF COWL SHOCK	THROAT	2D/3D RATIO
2D	0.370	0.108	0.038	1.31
3D	0.329	0.082	0.029	

Table 1. Mass Averaged Total Pressure Recovery

IV. CONCLUDING REMARKS

The present study is a preliminary investigation into the behavior of the flow within a 28 degree total geometric turning angle hypothetical Mach 10 inlet as calculated with the full three-dimensional Navier-Stokes equations. Comparison between the 2D and 3D solutions have been made. The overall compression is not significantly different between the 2D and center plane 3D solutions. Approximately one-half to two-thirds of the inlet flow at the exit of the inlet behave nominally two-dimensionally. On the other hand, flow field non-uniformities in the three-dimensional solution indicate the potential significance of the sidewall boundary layer flows ingested into the inlet.

The tailoring of the geometry at the inlet shoulder and on the cowl obtained in the 2D parametric design study have also proved to be effective at controlling the boundary layer behavior in the 3D code. The 3D inlet solution remained started indicating that the 2D design had a sufficient margin to allow for three-dimensional flow field effects. Although confidence is being gained in the use of SCRAM3D as applied to similar flow fields, the actual effects of the three-dimensional flow fields associated with sidewalls and wind tunnel installations can require verification with ground-based experiments.

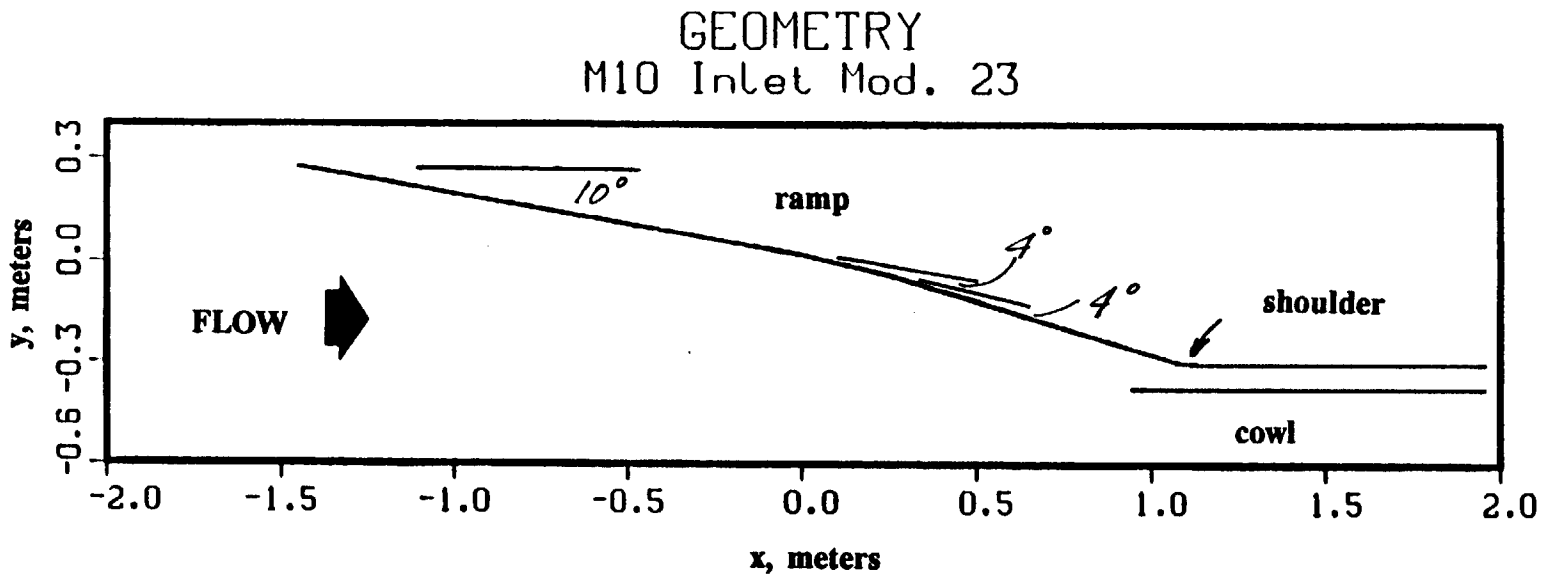

FIGURE 1. **Geometry for 36 degree inlet having a straight cowl and straight ramp.**

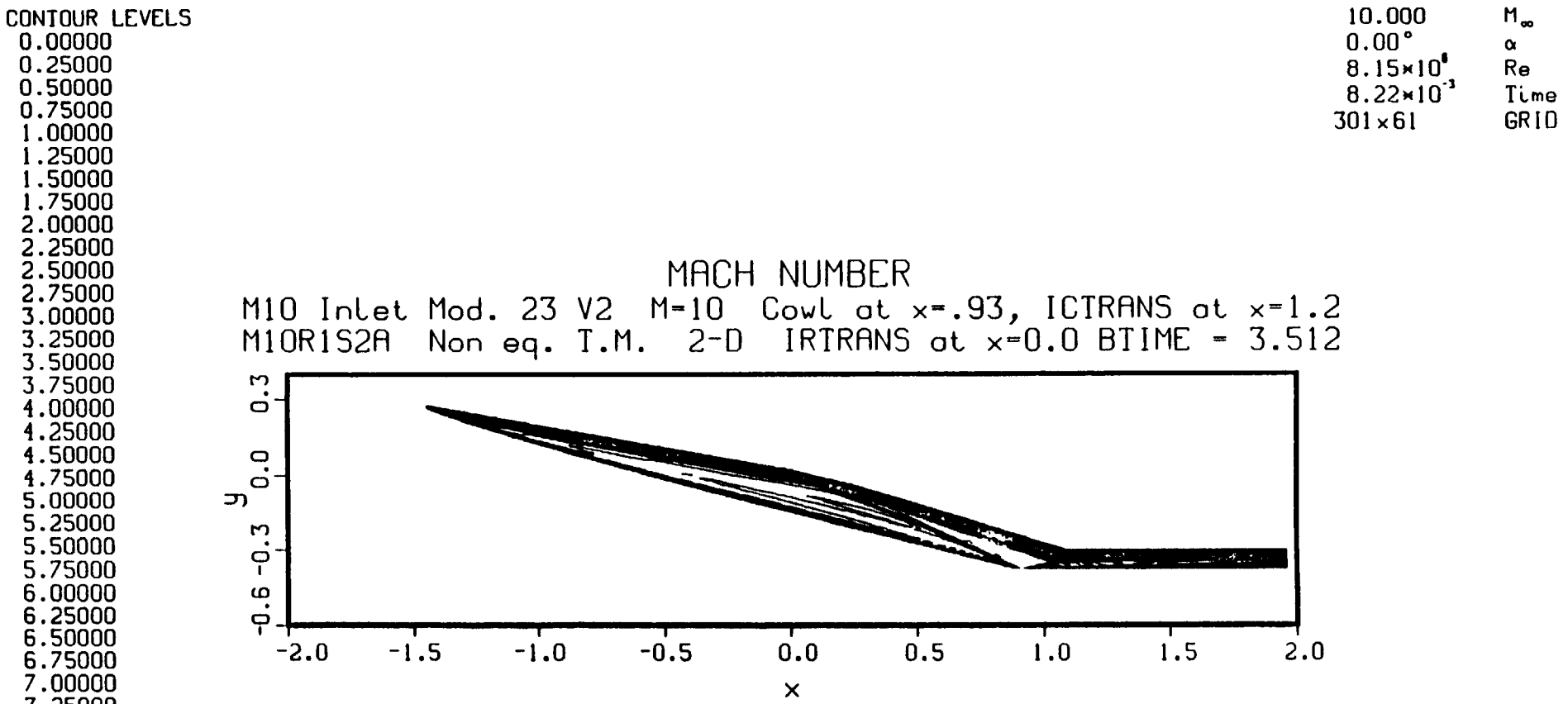

FIGURE 2. **Flow solution for 36 degree inlet with straight ramp and cowl at M=10.**

(a) Mach number contours shown to correct vertical and streamwise scales.

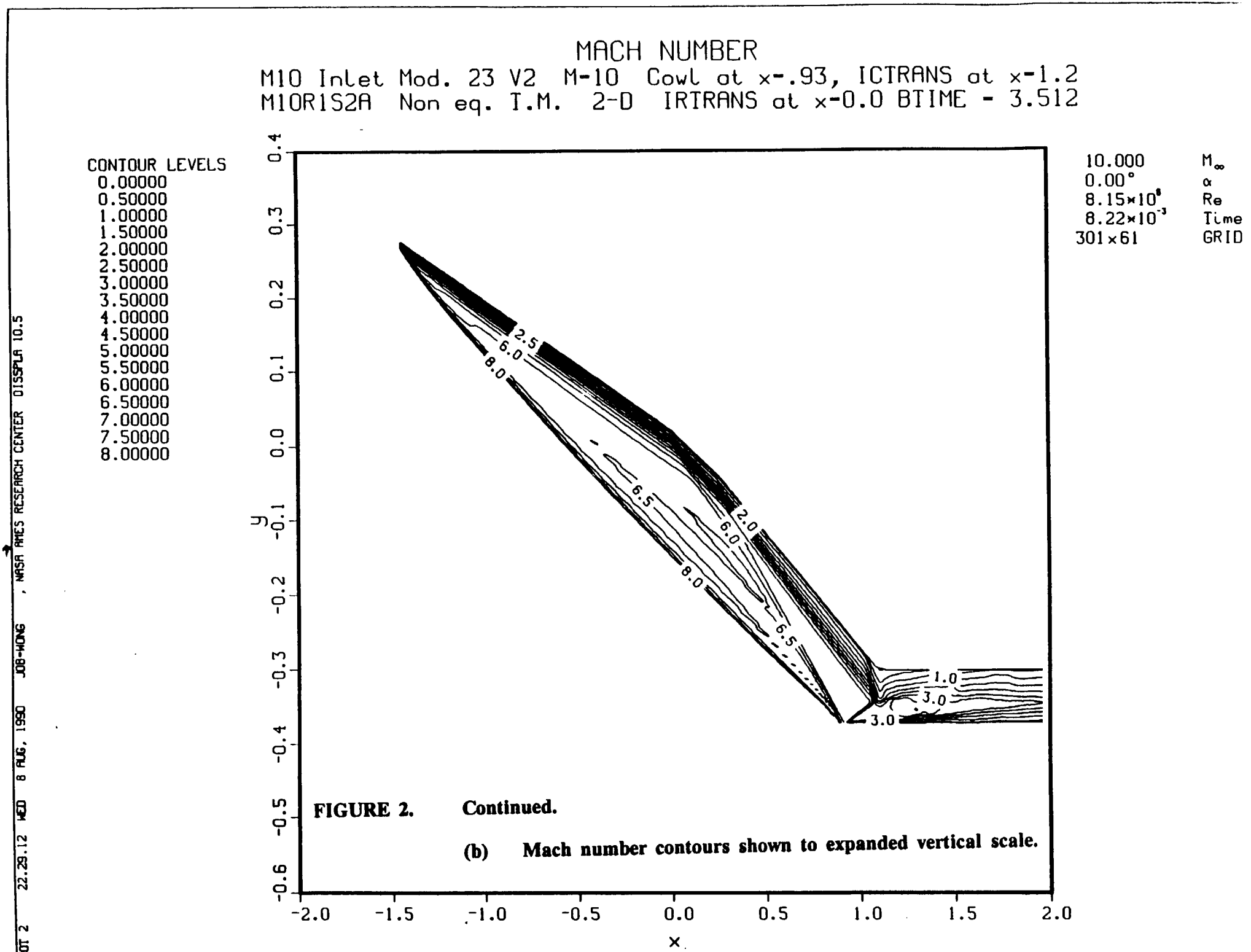

FIGURE 2. **Continued.**

(b) Mach number contours shown to expanded vertical scale.

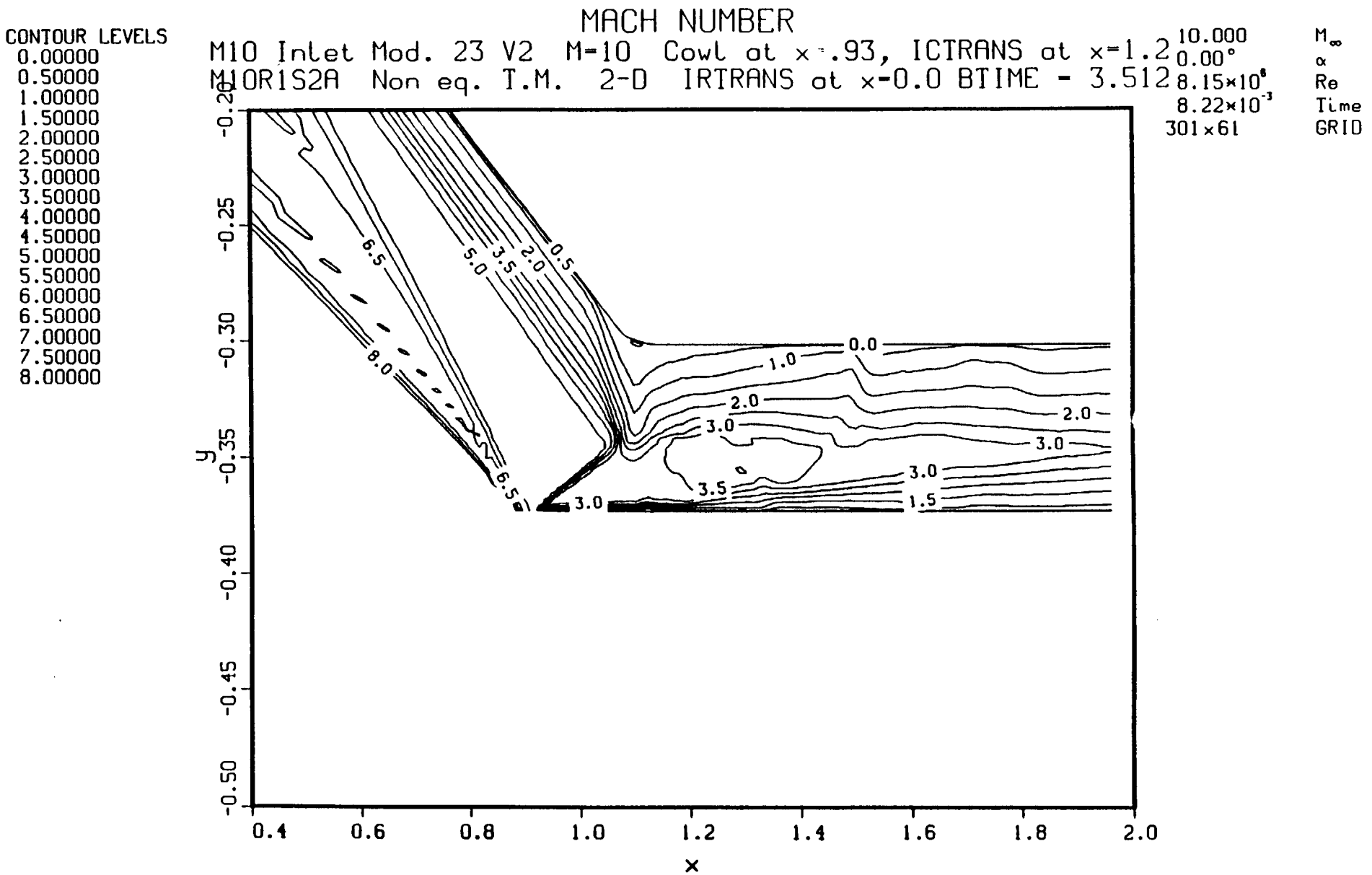

FIGURE 2. Continued.

(c) Mach number contours shown enlarged to indicate detail in throat region.

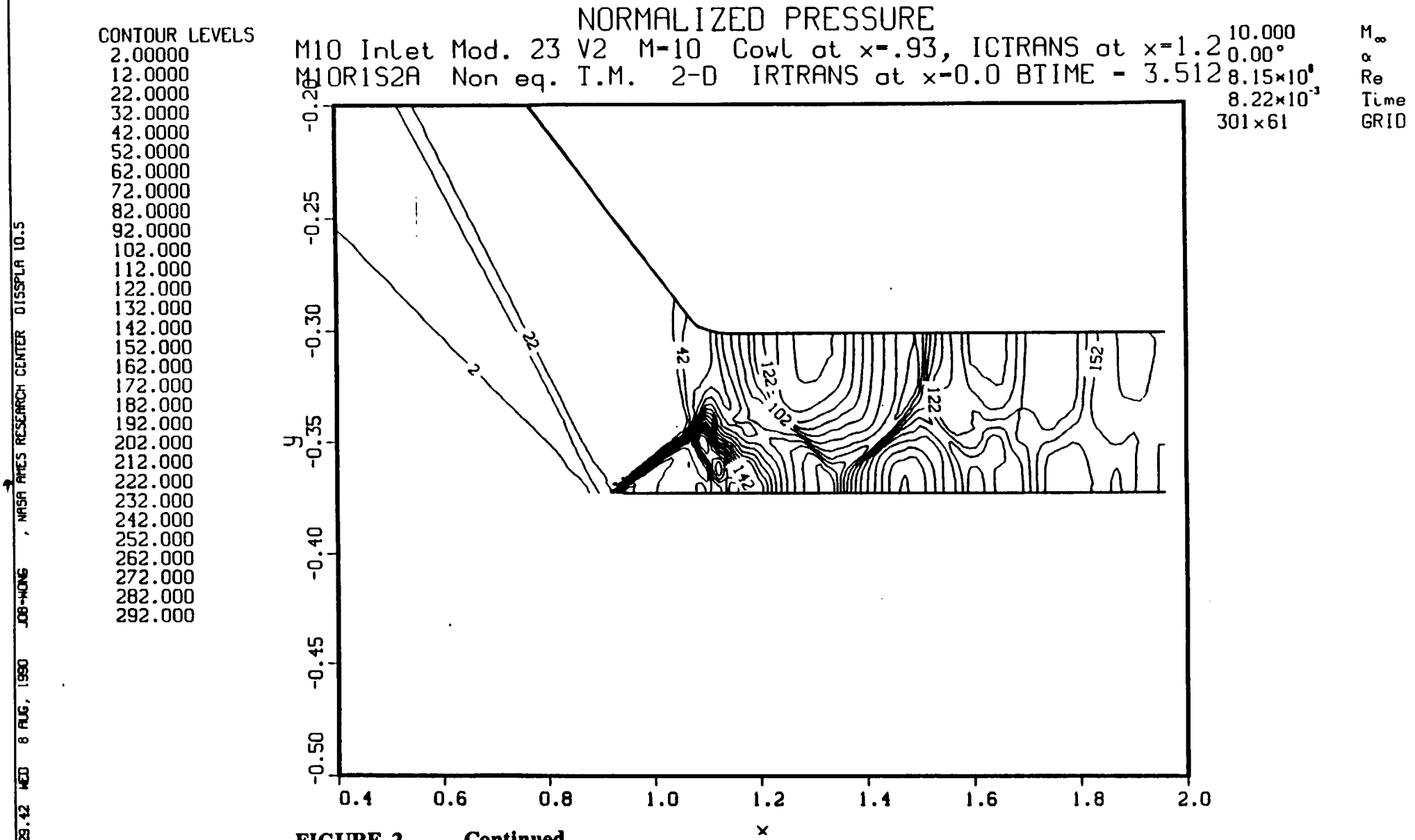

FIGURE 2. Continued.

(d) Pressure contours in throat region.

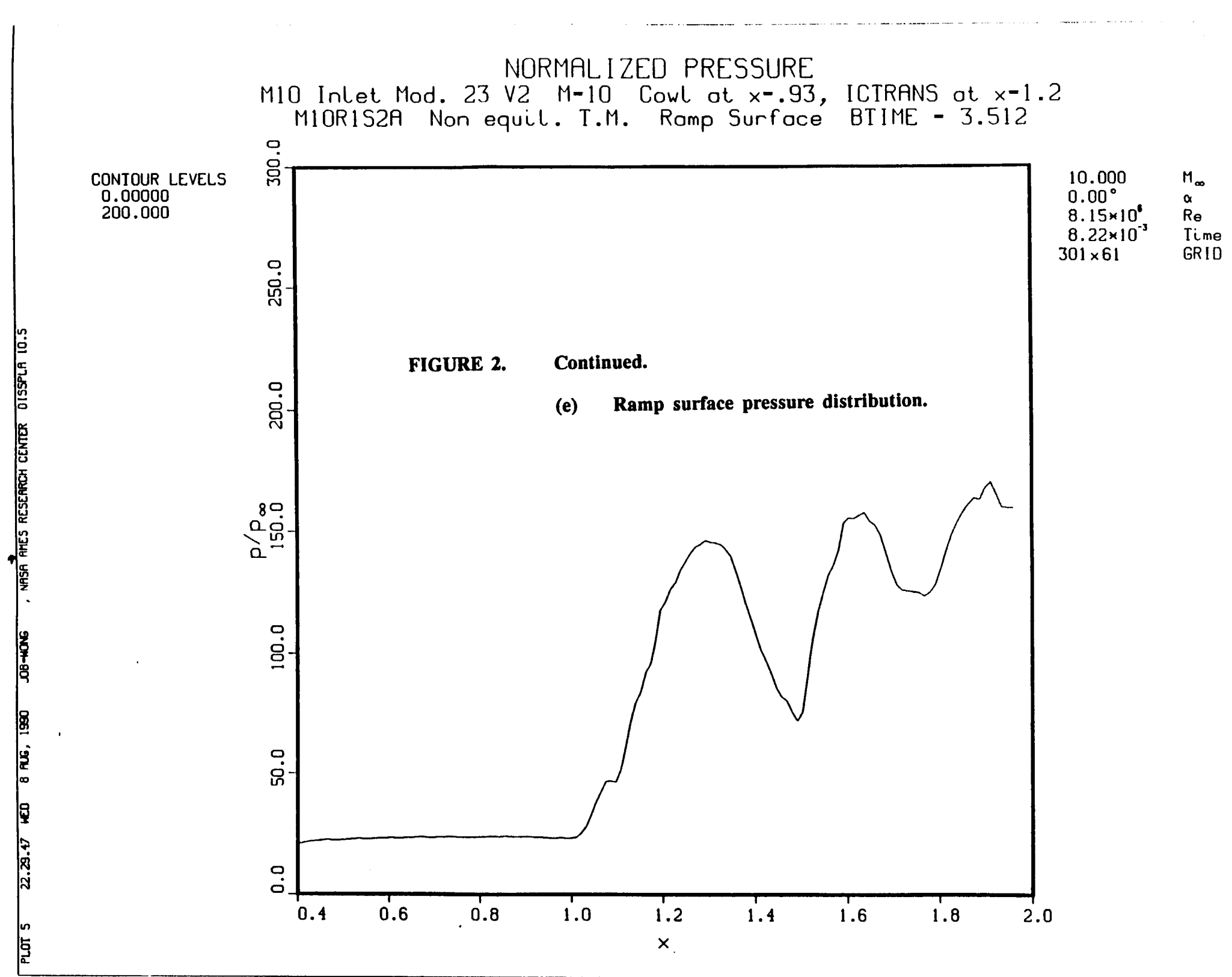

FIGURE 2. Continued.

(e) Ramp surface pressure distribution.

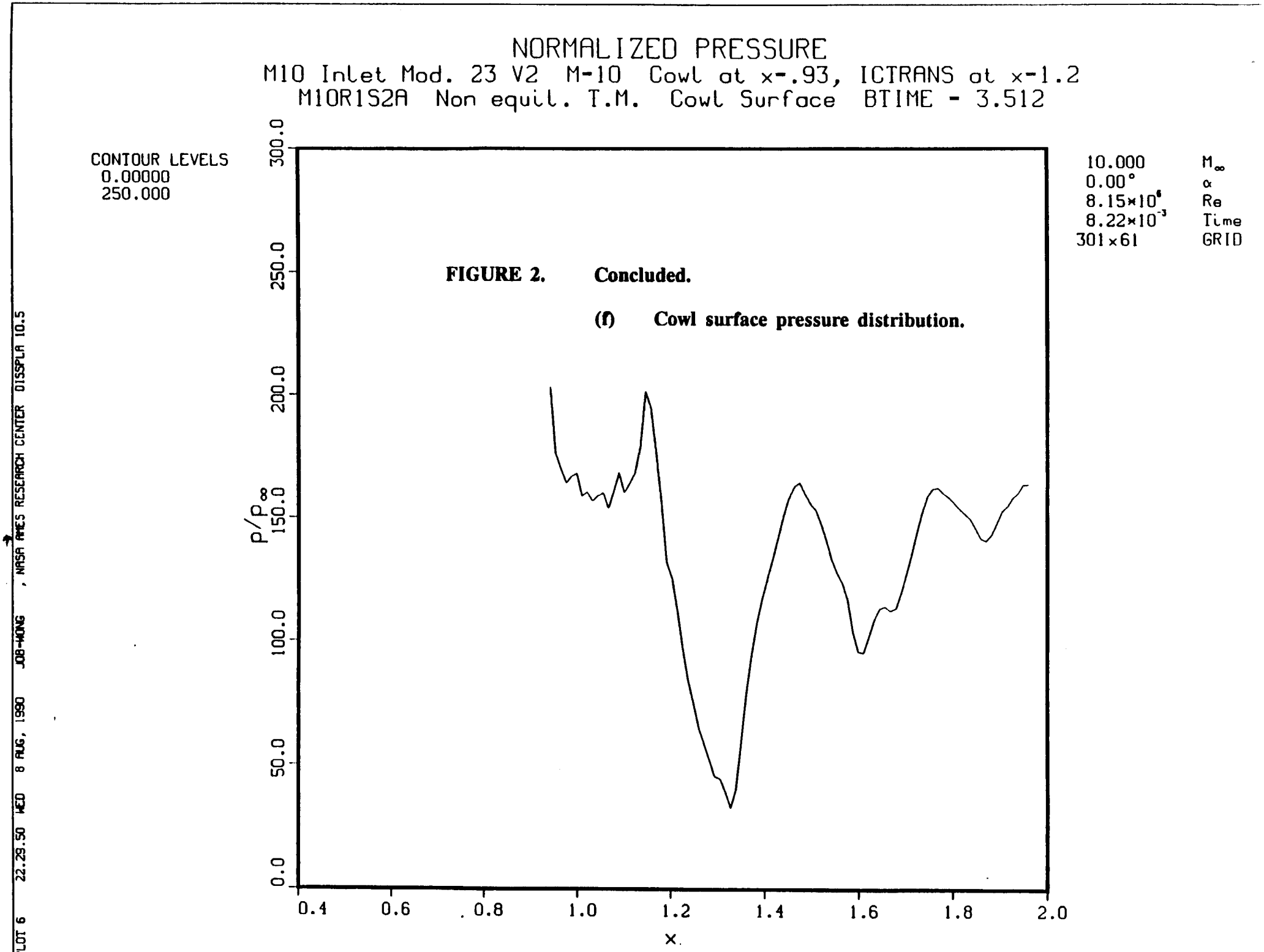

FIGURE 2. Concluded.

(f) Cowl surface pressure distribution.

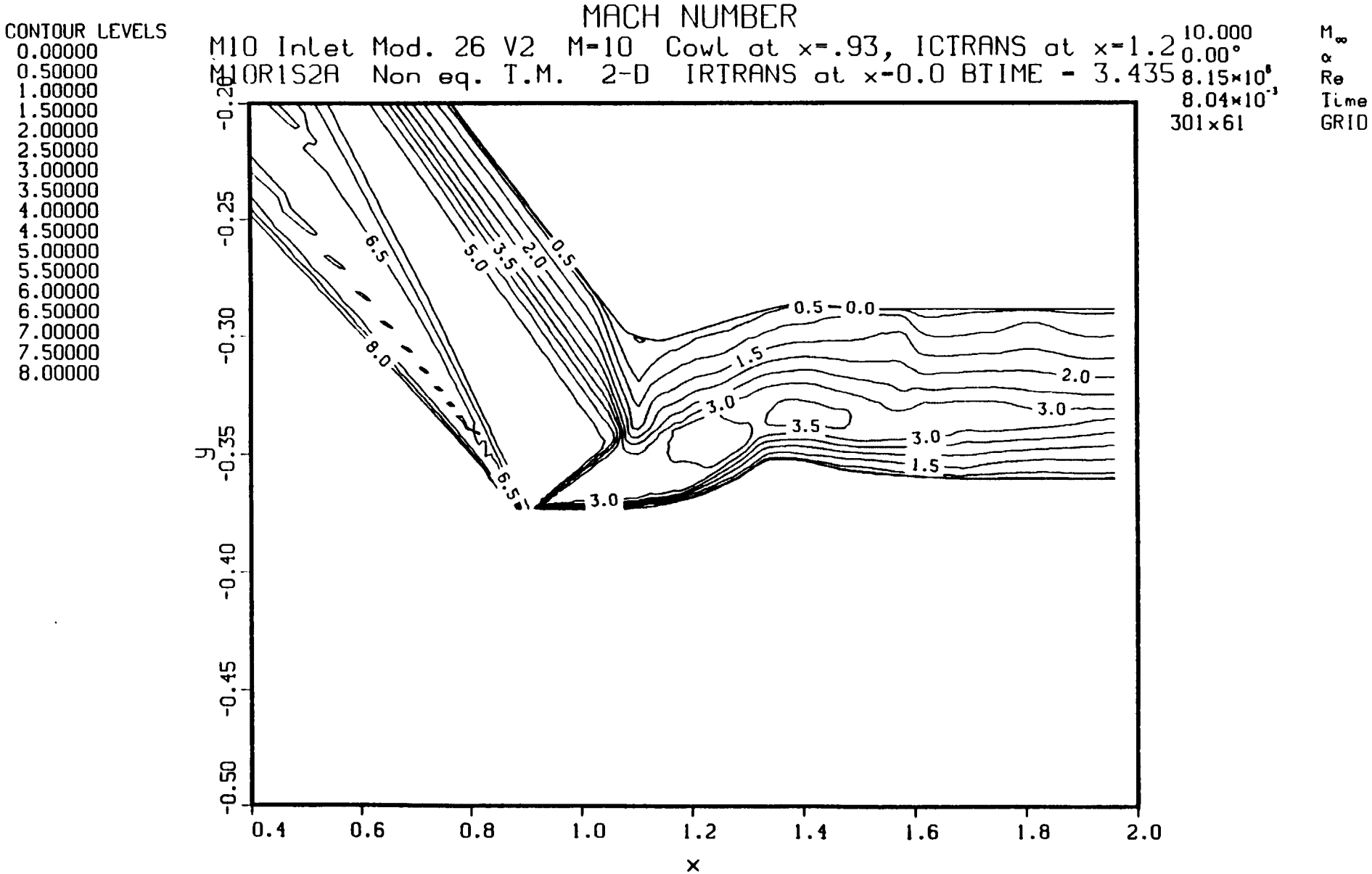

FIGURE 3. **Flow solution for 36 degree inlet with contoured ramp and cowl surfaces at M=10.**

(a) Mach number contour detail in throat region.

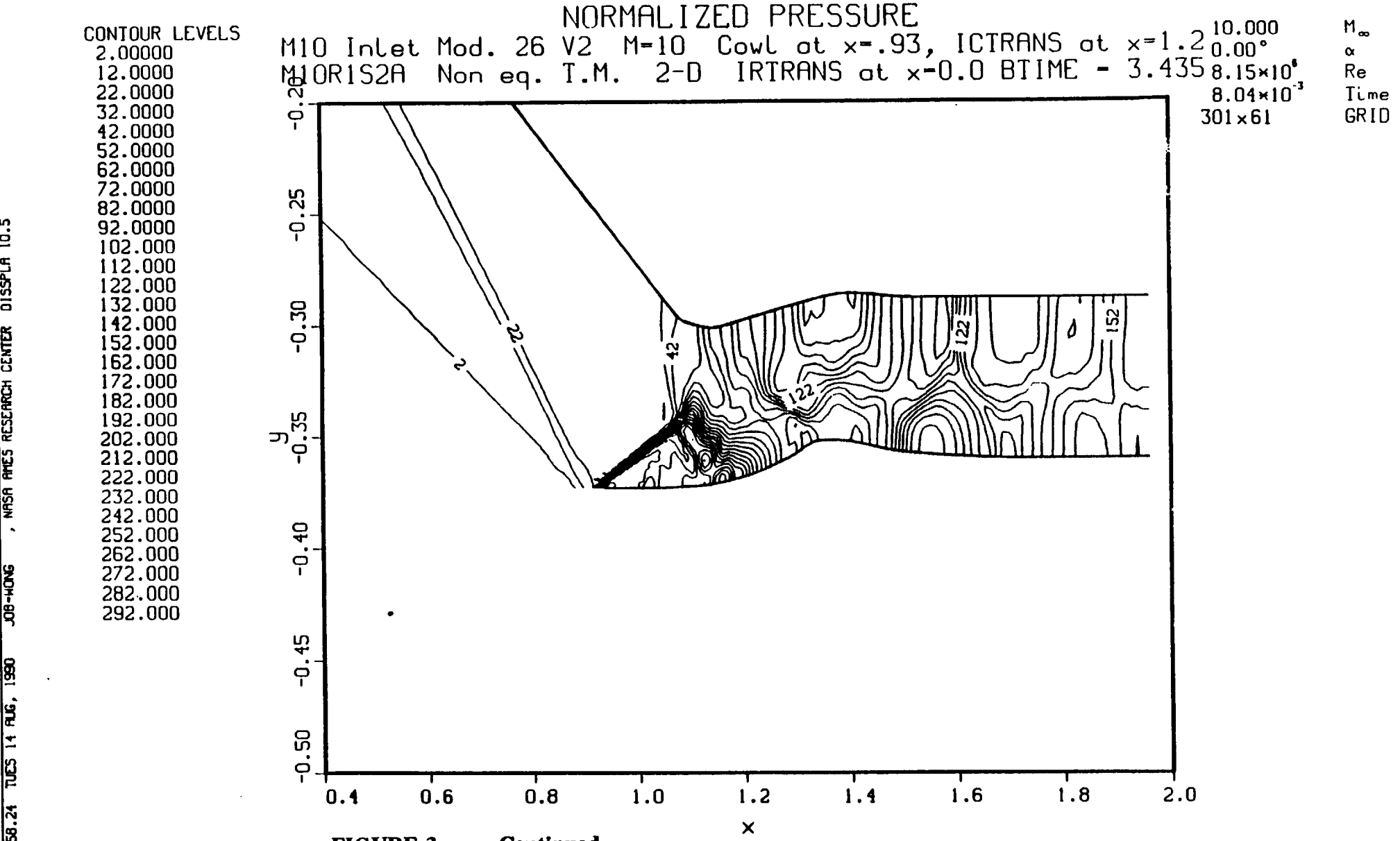

FIGURE 3. Continued.

(b) Pressure contours in throat region.

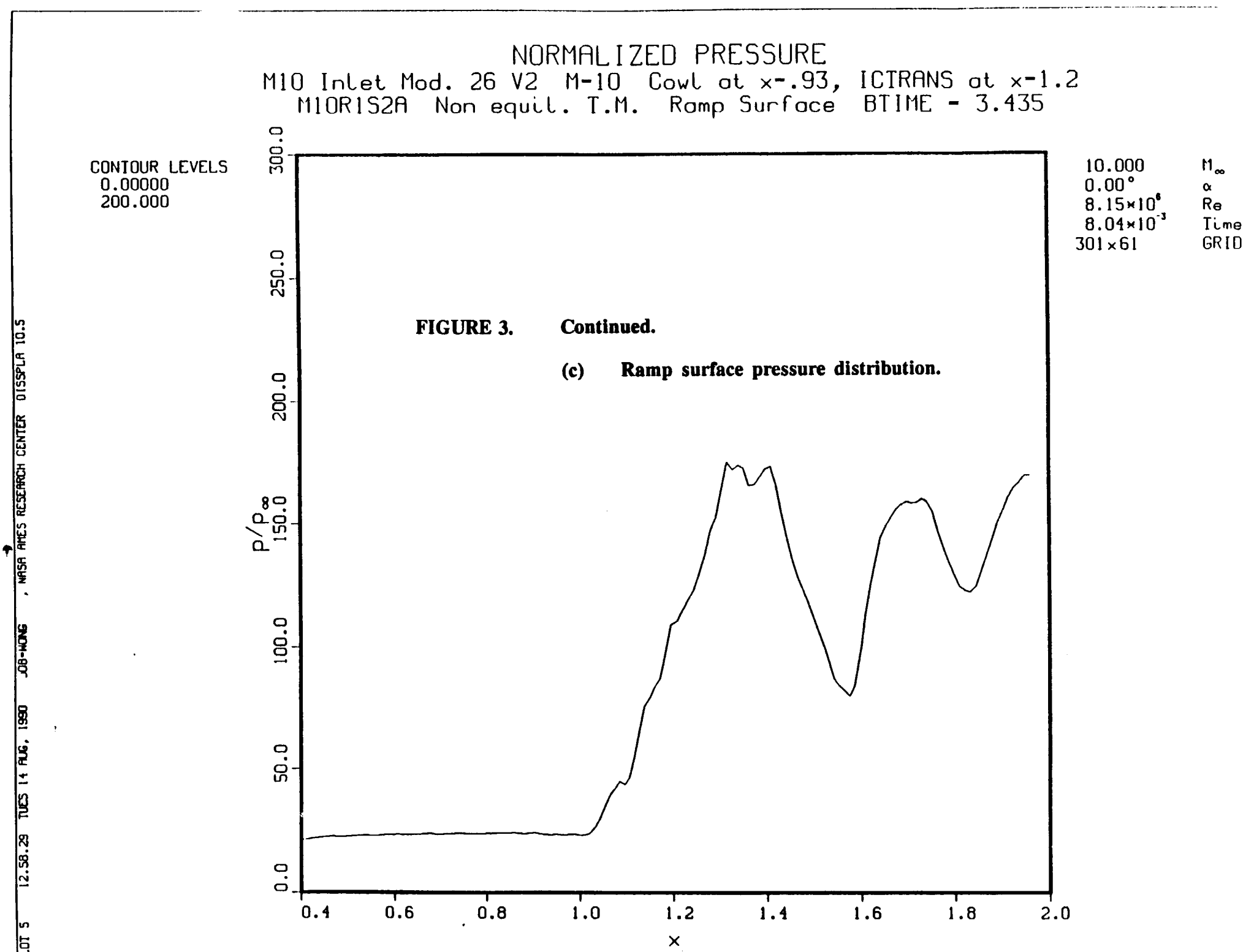

FIGURE 3. Continued.

(c) Ramp surface pressure distribution.

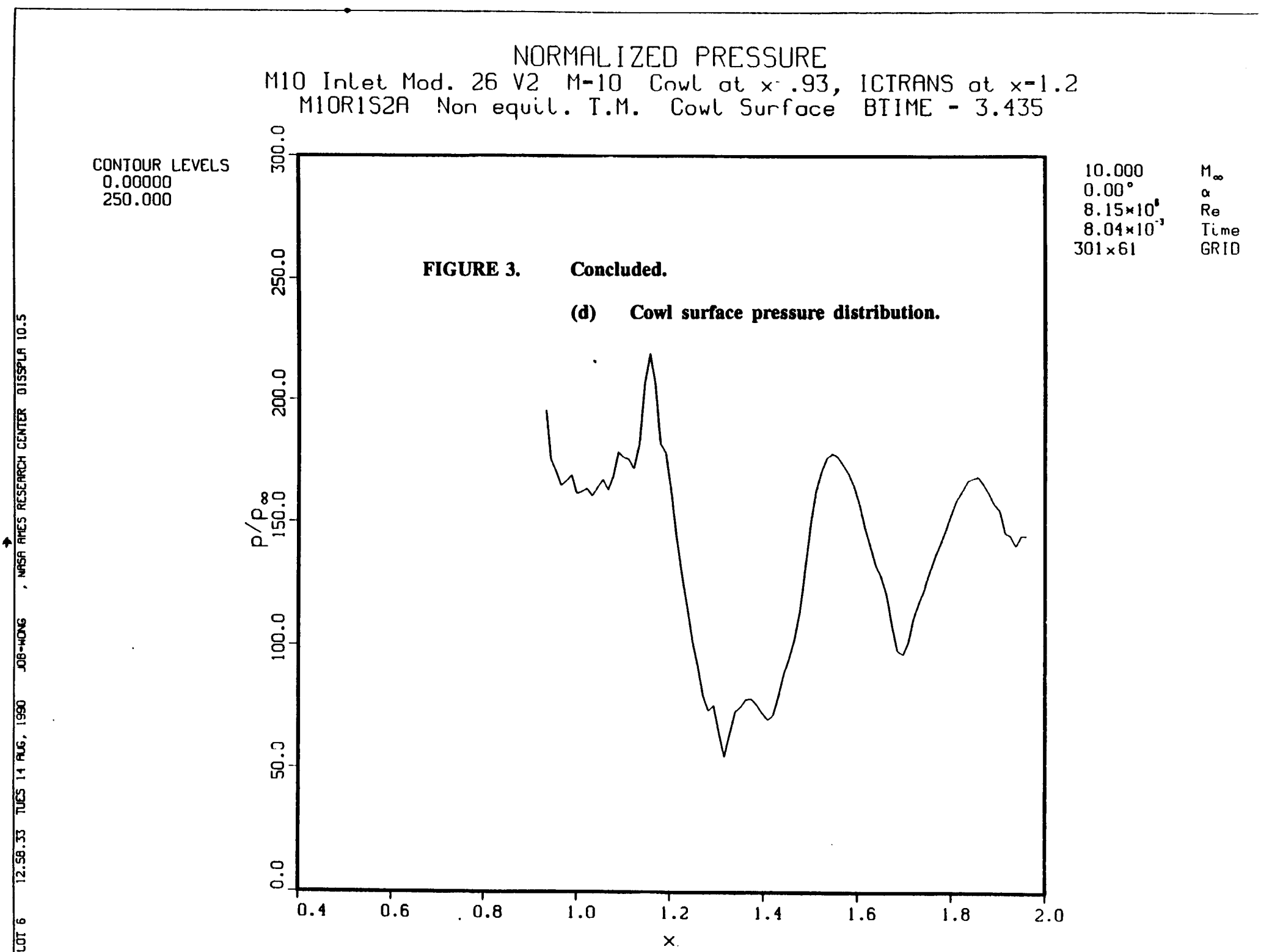

FIGURE 3. Concluded.

(d) Cowl surface pressure distribution.

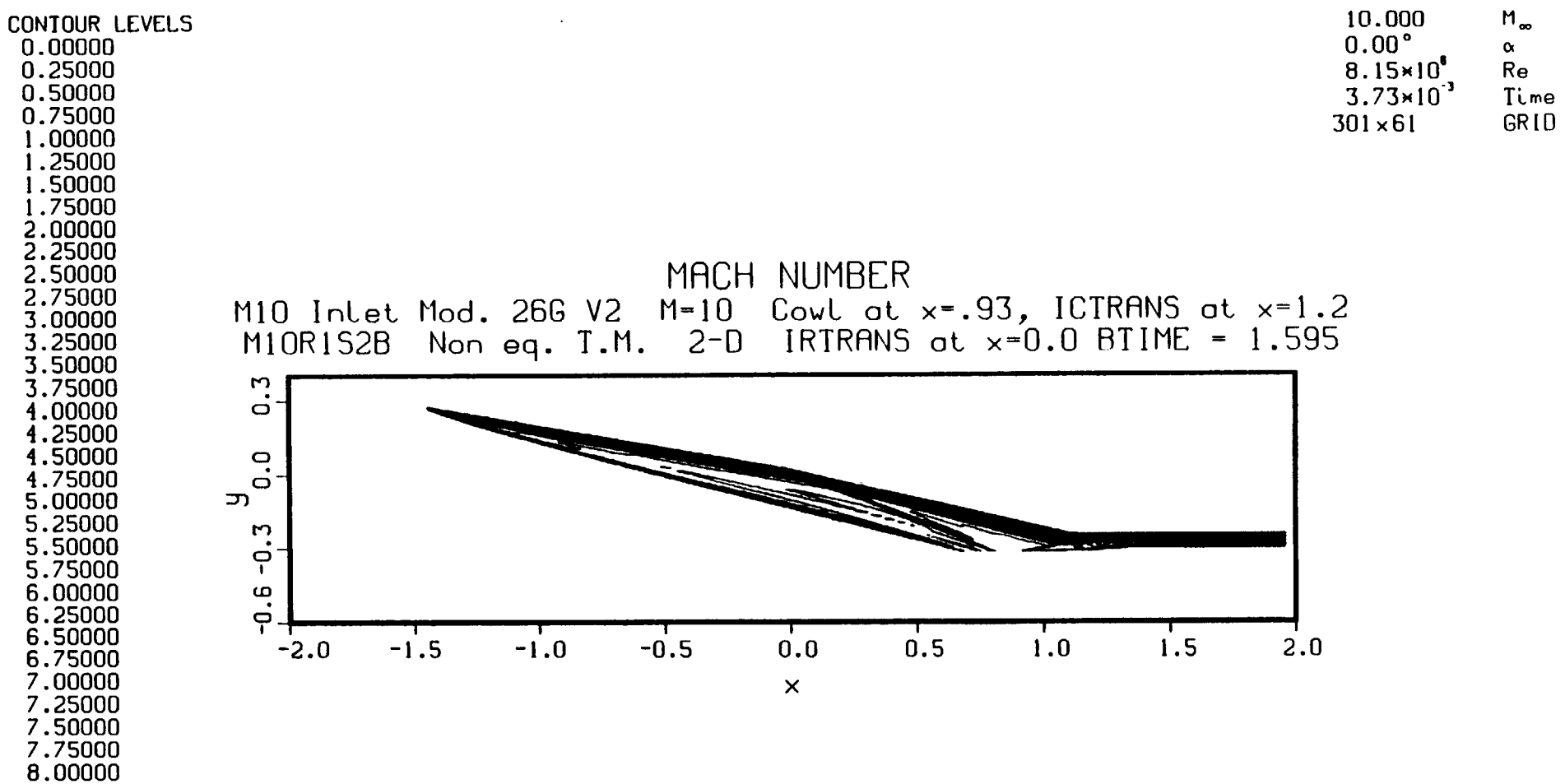

FIGURE 4. Flow solution for 28 degree inlet with rounded ramp shoulder and contoured cowl surface at M-10.

(a) Mach number contours shown to correct geometric scale.

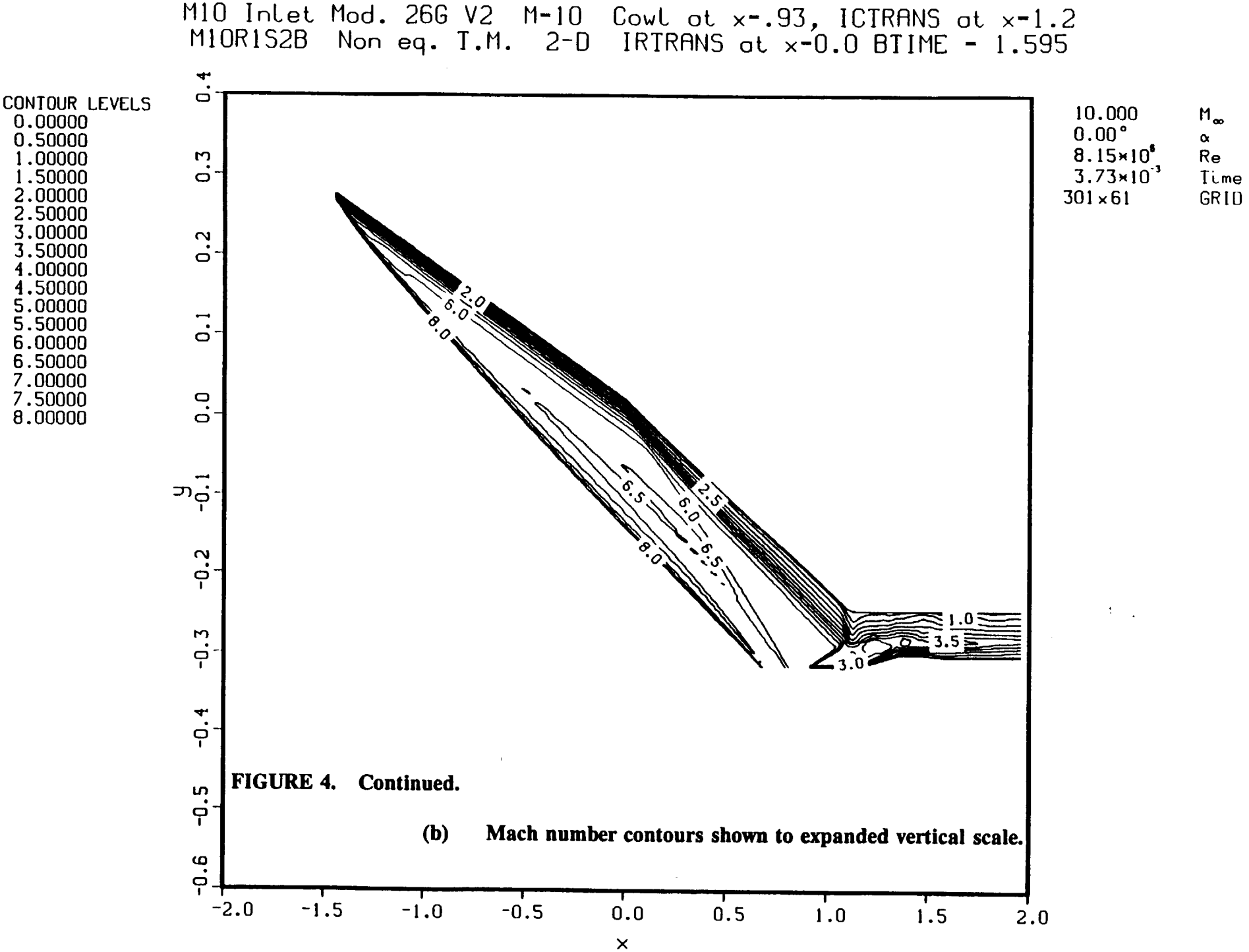

FIGURE 4. Continued.

(b) Mach number contours shown to expanded vertical scale.

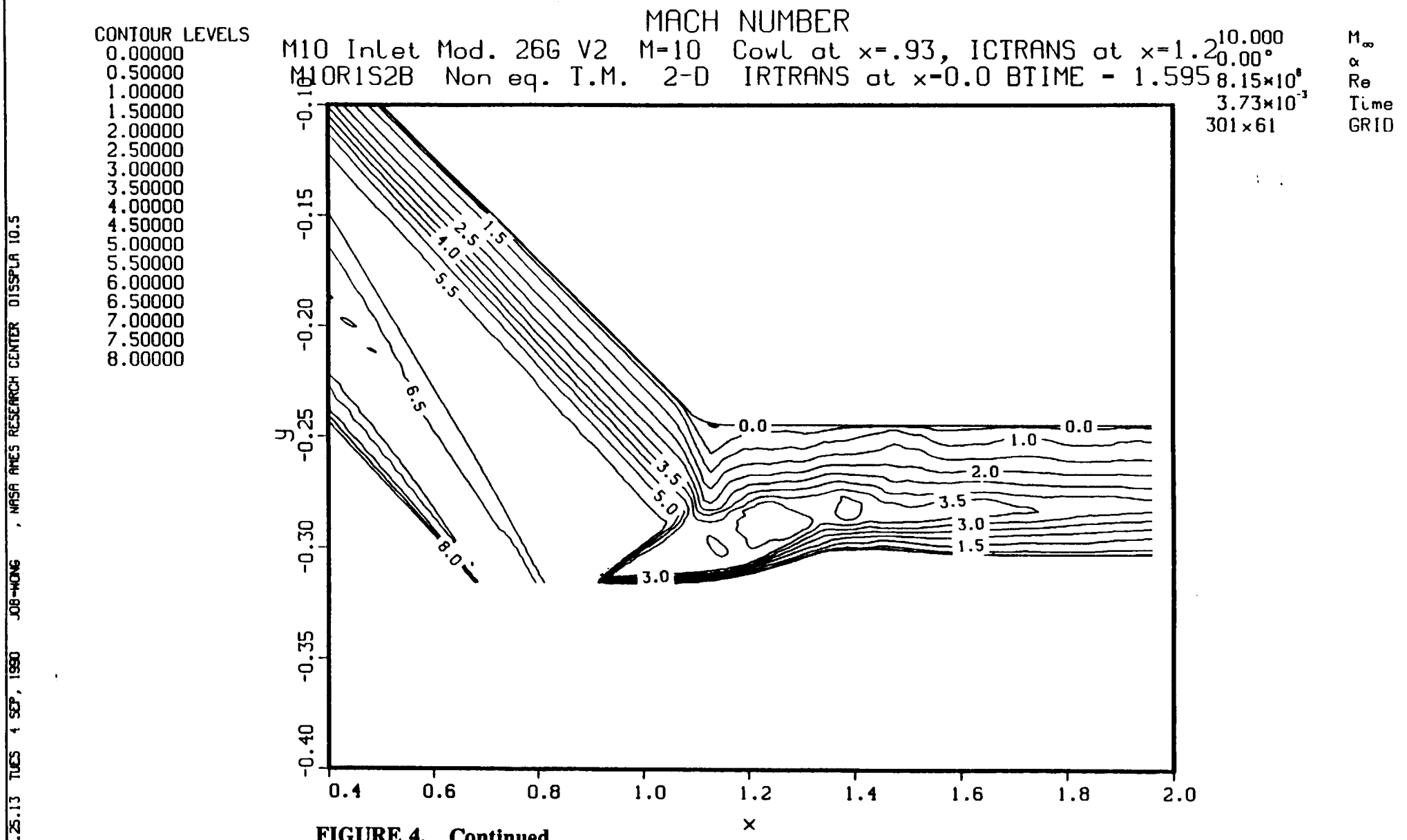

FIGURE 4. Continued.

(c) Mach number contour detail in throat region.

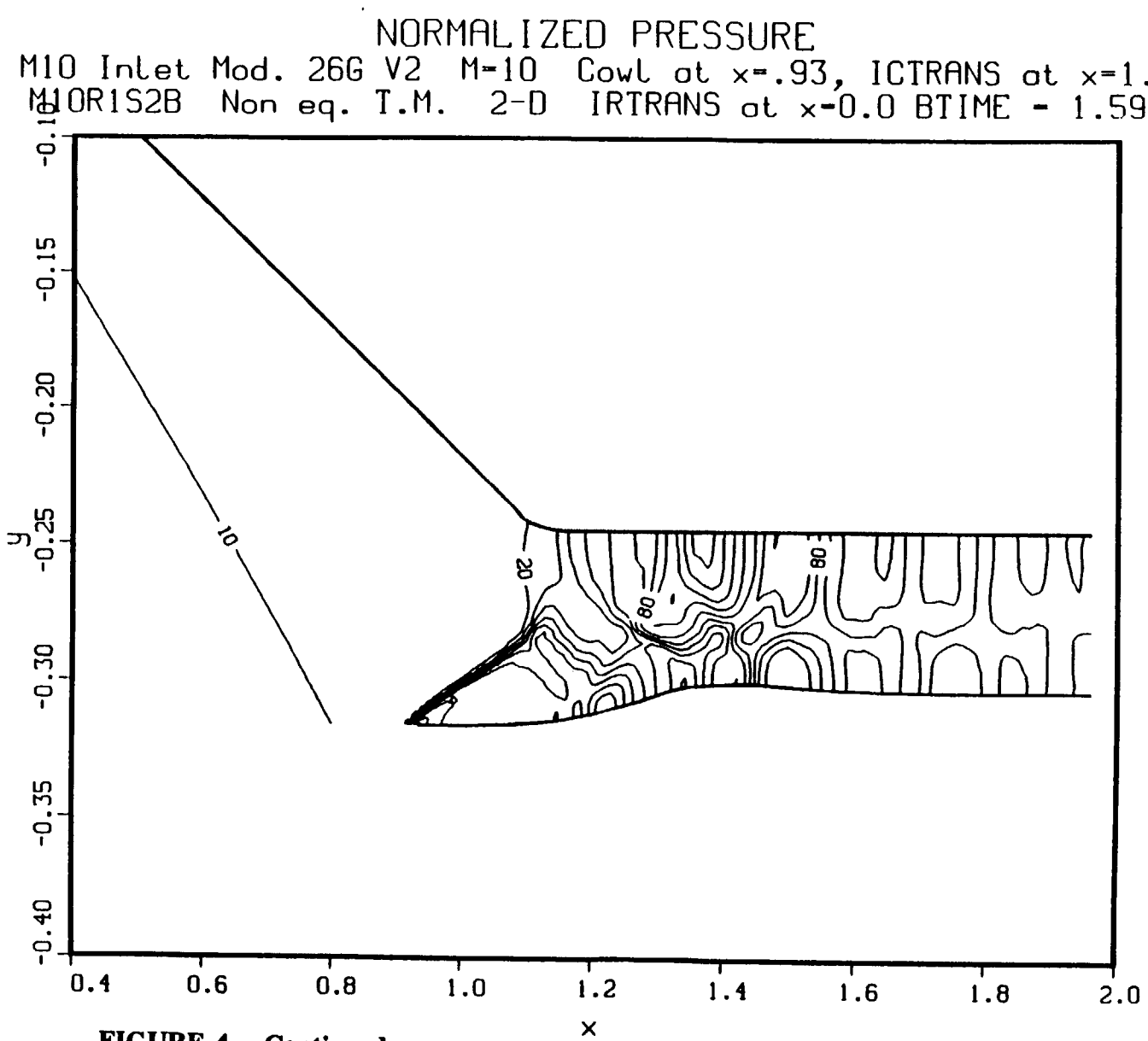

FIGURE 4. Continued.

(d) Pressure contours in throat region.

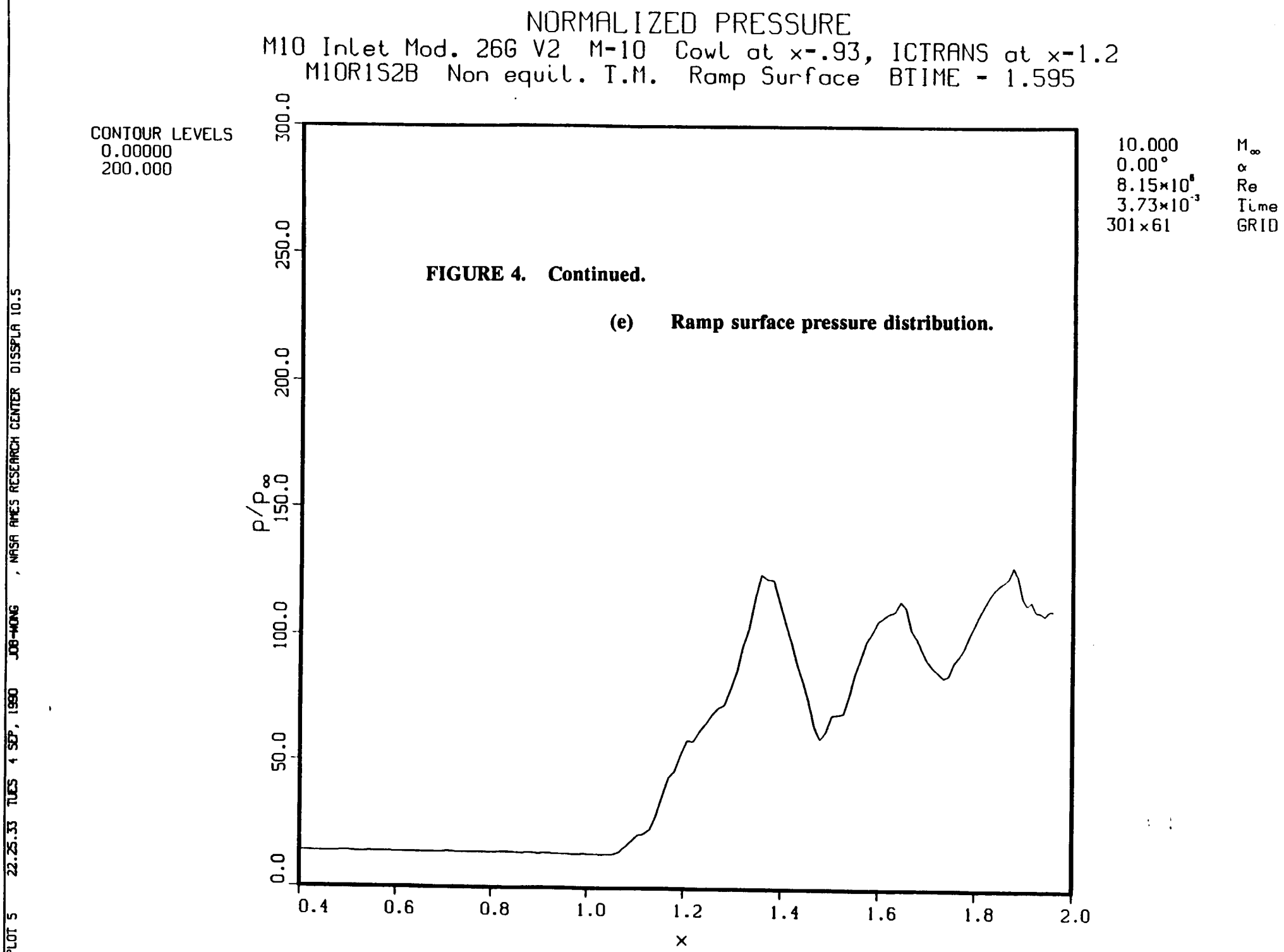

FIGURE 4. Continued.

(e) Ramp surface pressure distribution.

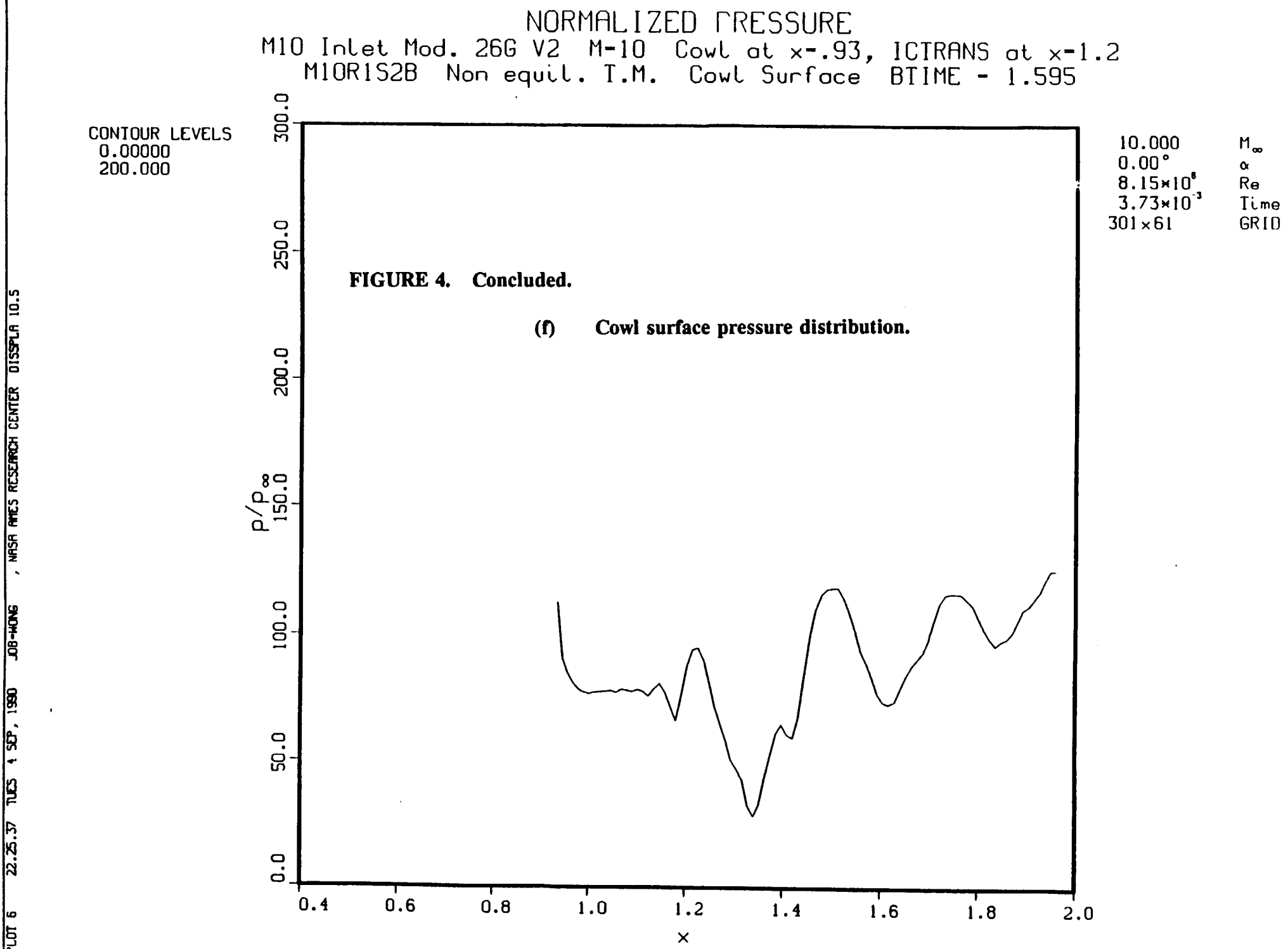

FIGURE 4. Concluded.

(f) Cowl surface pressure distribution.

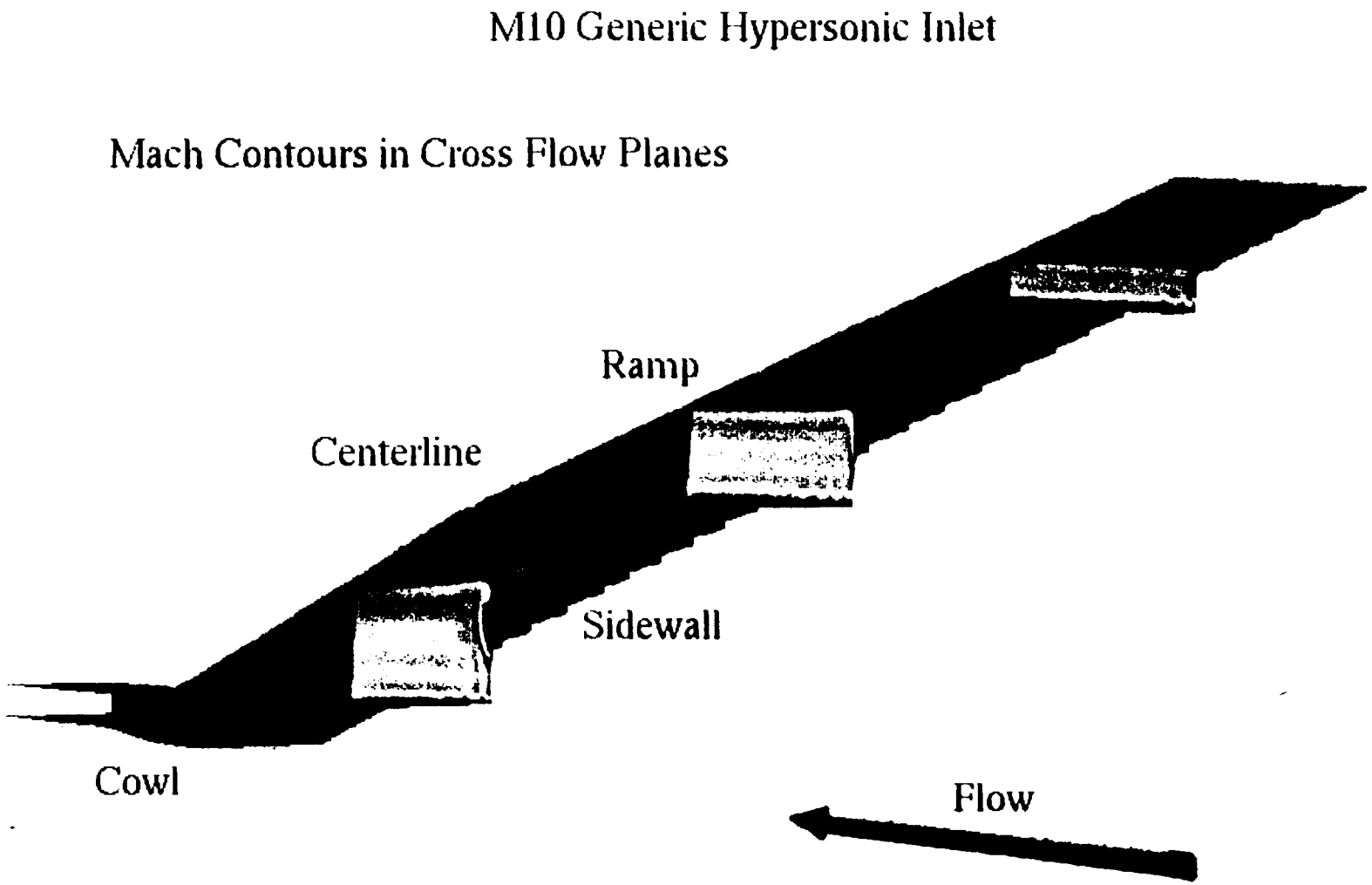

FIGURE 5. Surfaces used in three-dimensional simulations showing ramp, cowl and swept sidewalls along with Mach number contours in three representative cross flow planes.

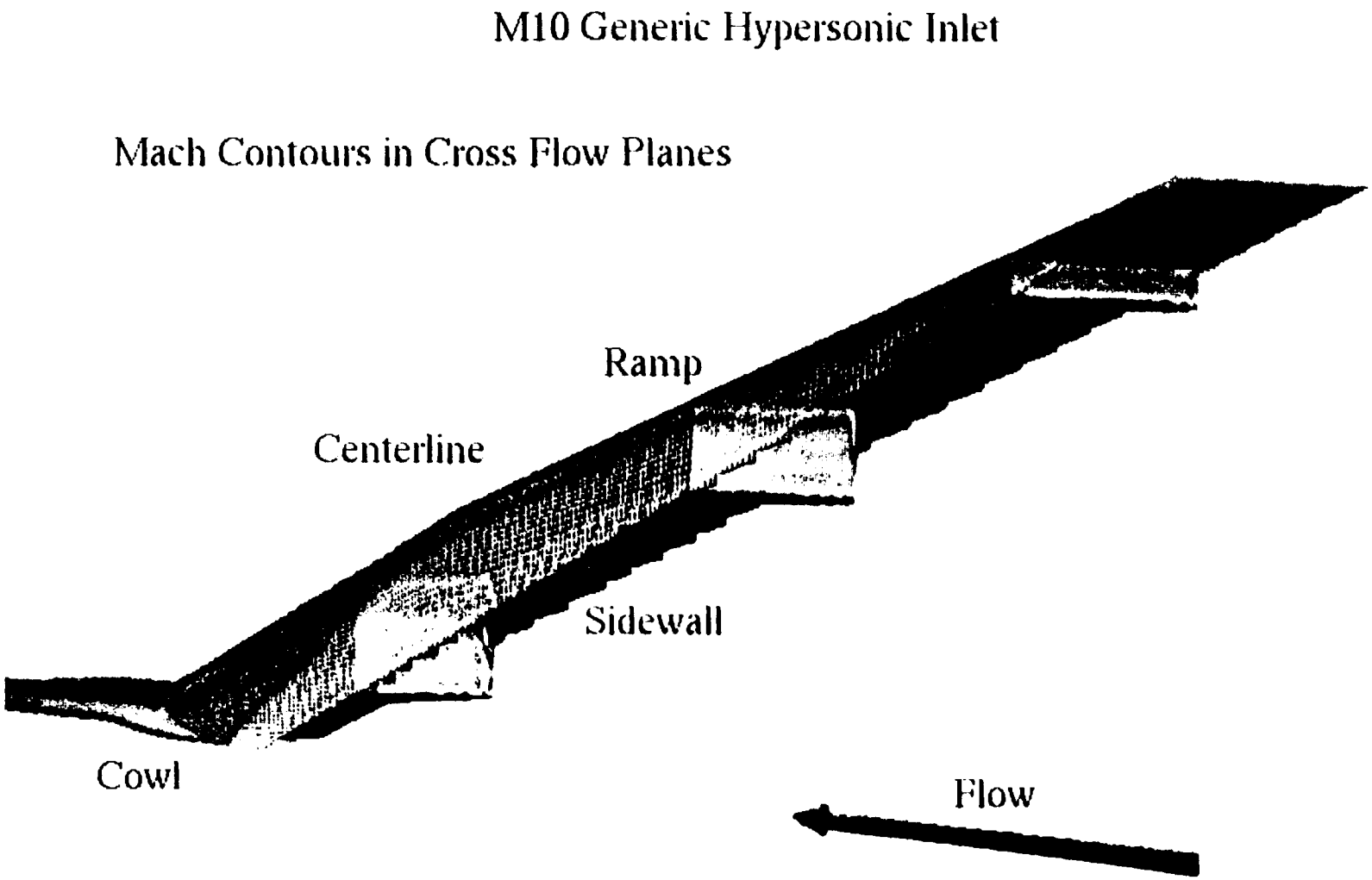

FIGURE 6. Three-dimensional solution showing Mach number contours on the center plane of the 3D calculation.

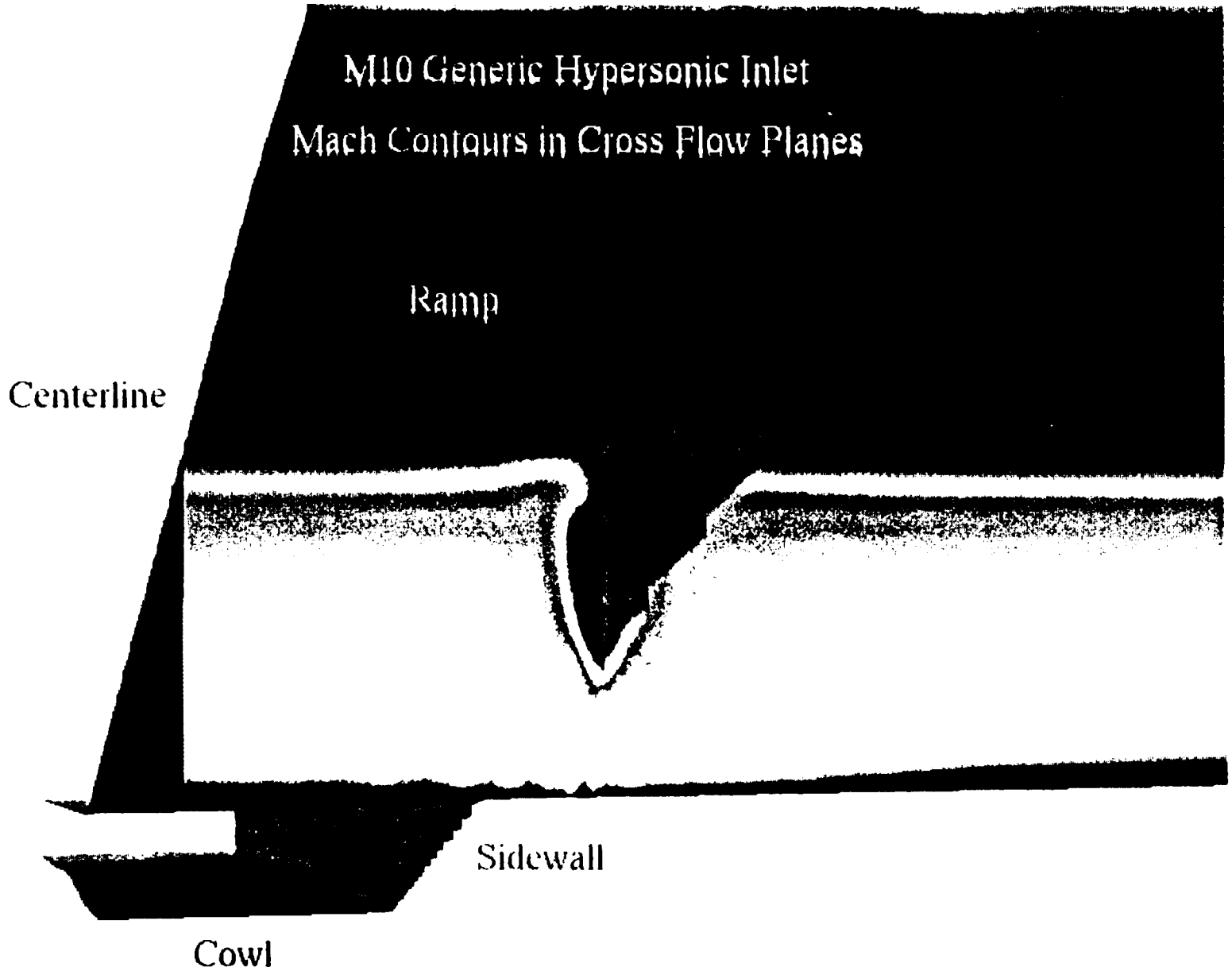

FIGURE 7. Mach number contours in cross flow plane just ahead of the cowl lip with outboard ramp present.

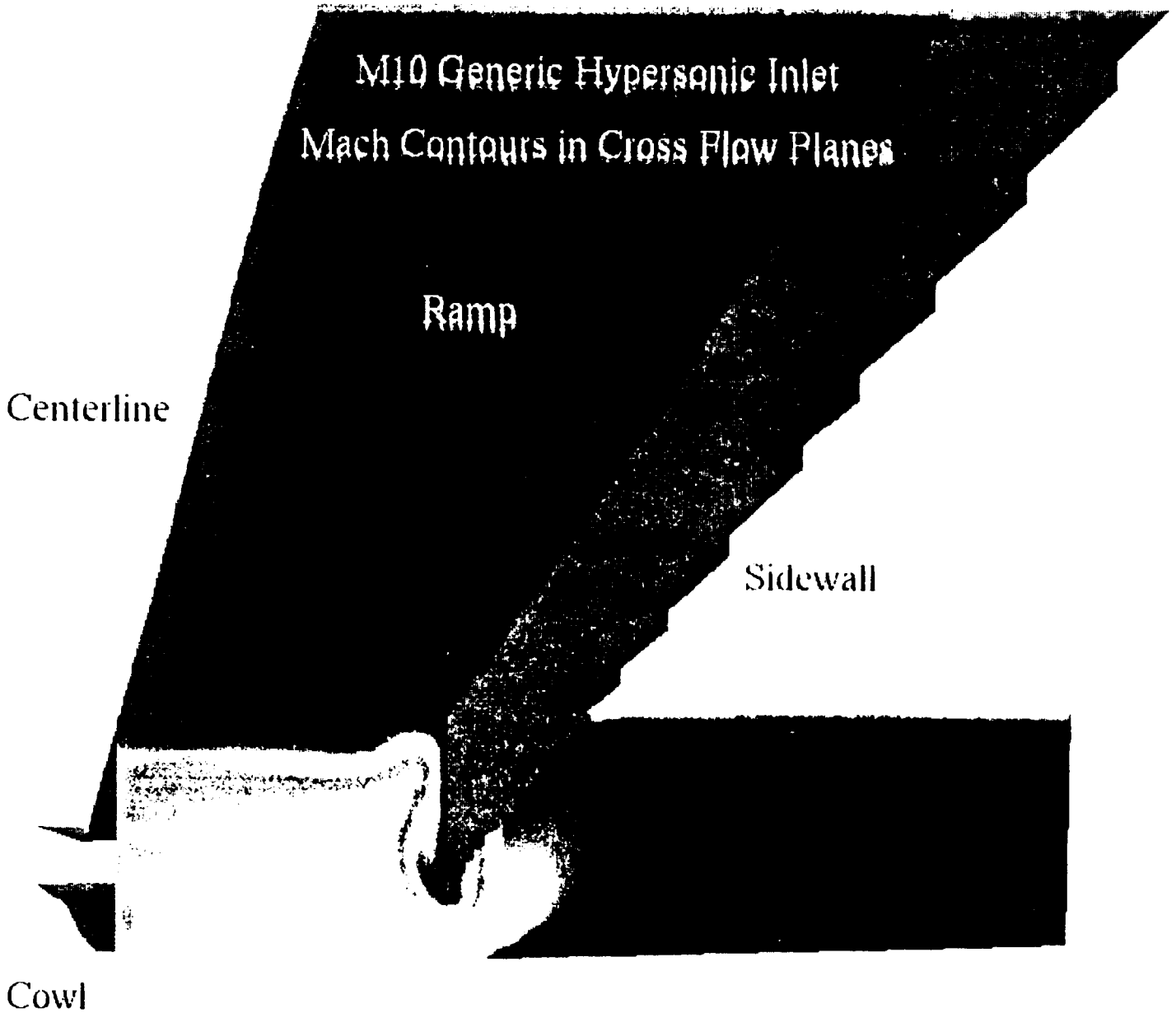

FIGURE 8. Mach number contours in cross flow plane just ahead of the cowl lip without outboard ramp.

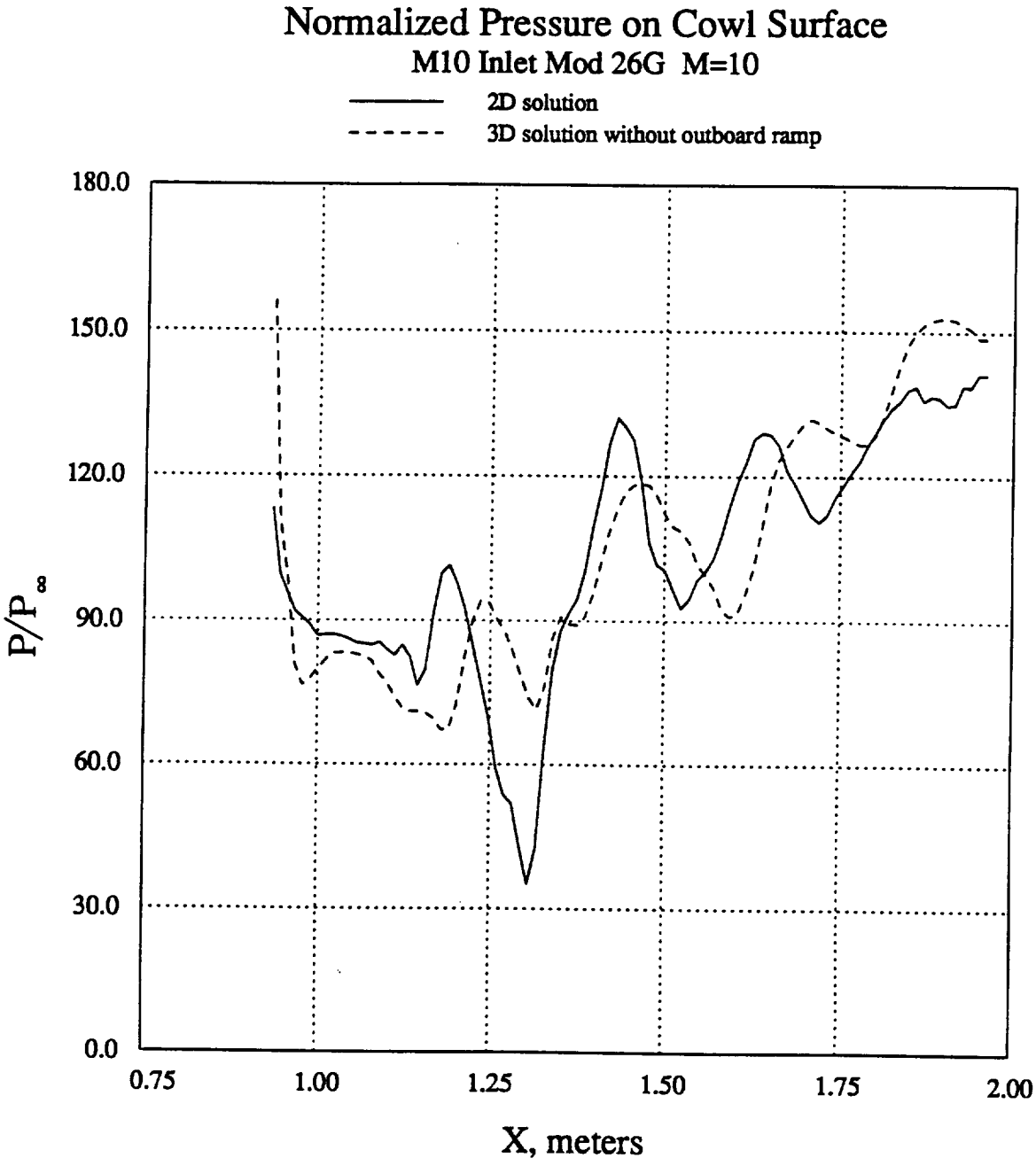

FIGURE 9. Concluded.

(b) Cowl surface pressure distribution.

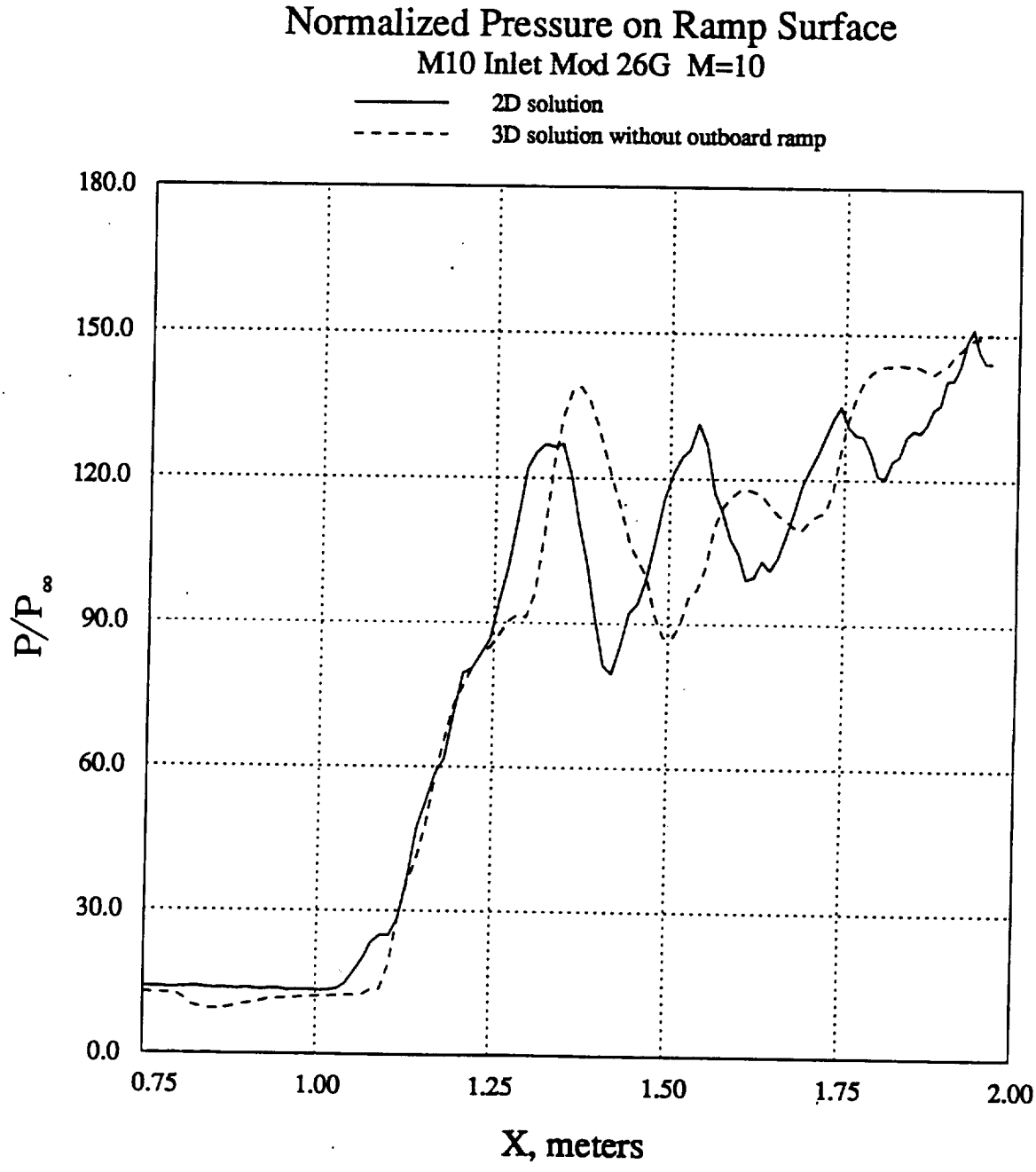

FIGURE 9. Comparison of two-dimensional and three-dimensional (center plane) pressures.

(a) Ramp surface pressure distribution.

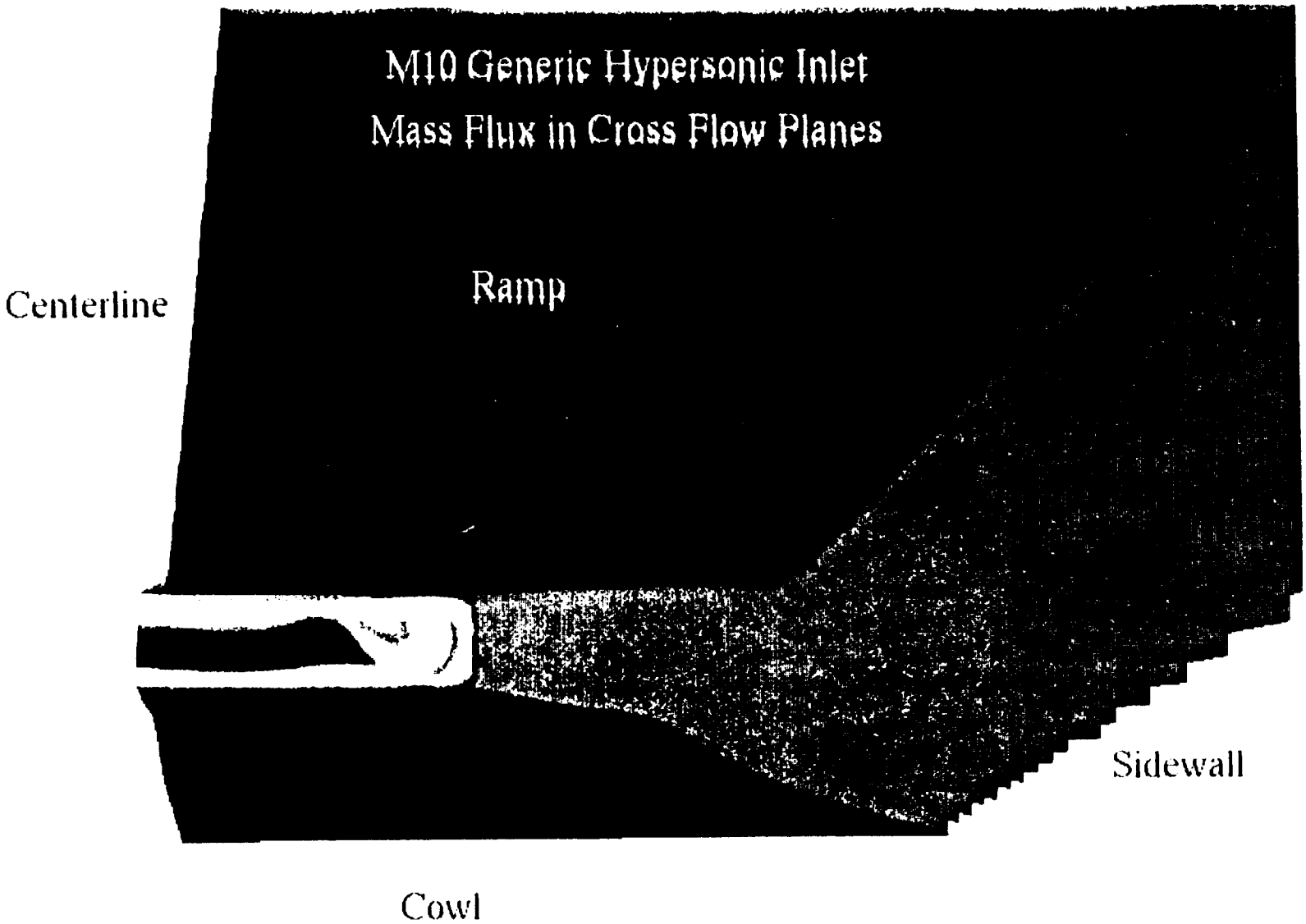

FIGURE 10. Mass flux contour at the exit of the inlet.